Carbon nanotubes as substrates for molecular spiropyran-based switches

E. Malic[1], A. Setaro[2], P. Blümmel[2], Carlos F. Sanz-Navarro[3], Pablo Ordejón[3], S. Reich[2], and A. Knorr[1]

[1] Institut für Theoretische Physik, Technische Universität Berlin, 10623 Berlin, Germany
[2] Fachbereich Physik, Freie Universität Berlin, 14195 Berlin, Germany
[3] Centre d'Investigació en Nanociència i Nanotecnologia (CIN2), Campus UAB, Bellaterra, Spain

E-mail: ermin.malic@tu-berlin.de

Abstract. We present a joint theory-experiment study investigating the excitonic absorption of spiropyran-functionalized carbon nanotubes. The functionalization is promising for engineering switches on molecular level, since spiropyrans can be reversibly switched between two different conformations inducing a distinguishable and measurable change of optical transition energies in the substrate nanotube. Here, we address the question whether an optical read-out of such a molecular switch is possible. Combining the density matrix and the density functional theory, we first calculate the excitonic absorption of pristine and functionalized nanotubes. Depending on the switching state of the attached molecule, we observe a red-shift of transition energies by about 15 meV due to the coupling of excitons with the molecular dipole moment. Then, we perform experiments measuring the absorption spectrum of functionalized carbon nanotubes for both conformations of the spiropyran molecule. We find a good agreement between the theoretically predicted and experimentally measured red-shift confirming the possibility for an optical read-out of the nanotube-based molecular switch.

PACS numbers: 78.67.Ch, 42.79.Ta, 71.35.Cc, 78.40.Ri

1. Introduction

The adsorption of molecules to the surface of carbon nanostructures is moving more and more into the focus of current research [1, 2, 3, 4, 5, 6, 7, 8, 9, 10, 11, 12, 13]. The functionalization of graphene and carbon nanotubes (CNTs) consisting of a single atom layer is a promising strategy to create new hybrid systems with distinct and externally controllable properties. In particular, the functionalization of CNTs with photochrome molecules, such as spiropyrans and azobenzenes, has sparked a large interest in both fundamental research and industry, since the arising hybrid nanostructures can be exploited for engineering switches on molecular level as well as high-efficiency photo-detectors with a tunable wavelength range [14, 2, 5, 7, 8, 10, 11, 12, 13]. First experiments have been realized illustrating a successful covalent and non-covalent functionalization of carbon nanotubes with spiropyran molecules [2, 5, 11]. In particular, Guo et al. have shown that spiropyran molecules can be used to externally and reversibly switch the conductance of a carbon nanotube transistor [5].

There are few theoretical studies investigating the properties of CNTs functionalized with photochrome molecules [8, 10, 15]. However, the key for designing and engineering novel devices based on hybrid nanostructures is a better microscopic understanding of the interaction between the adsorbed molecule and the substrate nanotube. In a previous work addressing the change in absorption spectra of spiropyran-functionalized CNTs, we have investigated different functionalization regimes. Our calculations have revealed a red-shift of transition energies in the range of 30 meV depending in particular on the molecular dipole moment and its orientation [13]. In this work, we present a joint theory-experiment study investigating the excitonic absorption of spiropyran-functionalized CNTs. We extend the theoretical model performing ab initio calculation on the geometrical relaxation of the adsorbed molecule on the surface of the CNT. This allows us to exactly determine the dipole moment of the entire hybrid nanostructure including its orientation with respect to the CNT axis. The resulting theoretical absorption spectrum of functionalized carbon nanotubes is compared with corresponding experimental observations.

2. Theoretical approach

In this work, we focus on non-covalently functionalized carbon nanotubes, where the influence of the attached spiropyran molecule on the electronic structure of the substrate CNT is small, i.e. the band structure and the wave function remain approximately unchanged [3]. As a result, it is sufficient to investigate the behavior of a pristine CNT located in a static dipole field induced by the attached molecules. Our approach is based on a combination between the density matrix (DM) and the density functional theory (DFT). The DM formalism is exploited to microscopically determine the excitonic absorption coefficient $\alpha(\omega)$ for arbitrary functionalized CNT. The DFT is applied to perform a geometrical relaxation of the adsorbed molecule on the surface of the substrate nanotube and to determine the functionalization parameters, such as the dipole moment, the dipole orientation, and the molecule distance from the CNT surface. These parameters are needed for the calculation of $\alpha(\omega)$ within the DM

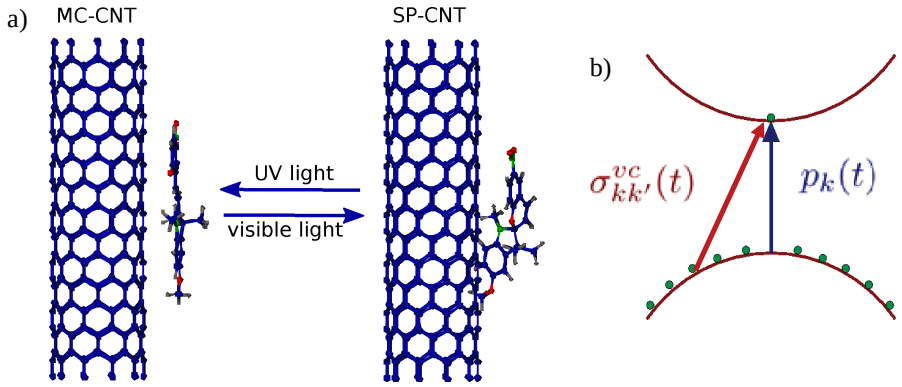

Figure 1. a) Spiropyran-functionalized exemplary (10,0) zigzag carbon nanotube. The attached molecule can be reversibly switched between the open merocyanine (MC) and the closed spiropyran (SP) conformation. The switching process is induced by visible and ultraviolet light, respectively. b) Schematic band structure of a CNT illustrating the inhomogeneous transitions $\sigma^{vc}_{kk'}$ and the microscopic polarization $p_k = \sigma^{vc}_{kk}$.

theory. Note that in this work we study the exciton-dipole interaction for a relatively small molecule density on the surface of the CNT making sure that there are no inter-molecular overlap effects.

The spiropyran molecules can be reversibly switched between the open merocyanine (MC) and the closed spiropyran (SP) conformation. The corresponding ring-opening/ring-closing process is driven by visible and ultraviolet light, respectively, cp. Fig. 1a. It induces a significant change of the molecular dipole moment enabling an externally stimulable coupling between the excitons in the CNT and the external dipole moment. As a result, depending on its conformation, the attached molecule accounts for a distinguishable and measurable change of the carrier mobility and the optical transitions in the substrate CNT.

The first step in our approach is the description of the many-particle Hamilton operator

$$H = H = H_0 + H_{c,f} + H_{c,c} + H_{c,d}\,, \tag{1}$$

which determines the dynamics of an carrier system described by: (i) the free-carrier part $H_0 = \sum_{\boldsymbol{l}} \varepsilon_{\boldsymbol{l}} a^+_{\boldsymbol{l}} a_{\boldsymbol{l}}$ with the electronic band structure $\varepsilon_{\boldsymbol{l}}$ [16, 17] and the ladder operators $a^+_{\boldsymbol{l}}$ and $a_{\boldsymbol{l}}$, which create and annihilate an electron in the state $\boldsymbol{l} = (k,\lambda)$ consisting of the momentum k along the CNT axis and the subband index λ, (ii) the coupling with a semi-classical electromagnetic field $H_{c,f} = i\hbar\frac{e_0}{m_0}\sum_{\boldsymbol{l}_1,\boldsymbol{l}_2} \boldsymbol{M}_{\boldsymbol{l}_1,\boldsymbol{l}_2} \cdot \boldsymbol{A}(t)\, a^+_{\boldsymbol{l}_1} a_{\boldsymbol{l}_2}$ with the optical matrix element $\boldsymbol{M}_{\boldsymbol{l}_1,\boldsymbol{l}_2}$ [18, 17, 19] and the vector potential $\boldsymbol{A}(t)$, (iii) the carrier-carrier interaction $H_{c,c} = \frac{1}{2}\sum_{\boldsymbol{l}_1,\boldsymbol{l}_2,\boldsymbol{l}_3,\boldsymbol{l}_4} V^{\boldsymbol{l}_1,\boldsymbol{l}_2}_{\boldsymbol{l}_3,\boldsymbol{l}_4}\, a^+_{\boldsymbol{l}_1} a^+_{\boldsymbol{l}_2} a_{\boldsymbol{l}_4} a_{\boldsymbol{l}_3}$ with the Coulomb matrix element $V^{\boldsymbol{l}_1,\boldsymbol{l}_2}_{\boldsymbol{l}_3,\boldsymbol{l}_4}$ [20, 19, 28], and (iv) the carrier coupling to the external molecular dipole moment

$$H_{c,d} = \sum_{\boldsymbol{l}_1,\boldsymbol{l}_2} g_{\boldsymbol{l}_1\boldsymbol{l}_2}\, a^+_{\boldsymbol{l}_1} a_{\boldsymbol{l}_2} \tag{2}$$

with the carrier-dipole coupling element $g_{\boldsymbol{l}_1\boldsymbol{l}_2} = \langle \Psi_{\boldsymbol{l}_1}(\boldsymbol{r}) | e_0 \phi_d(\boldsymbol{r}) | \Psi_{\boldsymbol{l}_2}(\boldsymbol{r}) \rangle$ with the zone-folded tight-binding wavefunctions $\Psi_{\boldsymbol{l}}(\boldsymbol{r})$ and the dipole potential $\phi_d(\boldsymbol{r}) = \frac{1}{4\pi\varepsilon_0}\frac{\boldsymbol{d}\cdot(\boldsymbol{r}-\boldsymbol{R}_d)}{|\boldsymbol{r}-\boldsymbol{R}_d|^3}$ [13]. The external dipole field depends on the dipole moment d, its orientation α with respect to the CNT axis, and its distance R_d from the CNT surface. These parameters are determined within

ab-initio calculations performed within the SIESTA package [21, 22] including the recently implemented Van der Waals exchange-correlation functional [23]. The calculation of the microscopic dipole moment of a fully relaxed spiropyran- and merocyanine-functionalized carbon nanotube is based on a recent technique considering finite CNTs built up by unit cell with Clar sextet edges terminated with hydrogen atoms [24]. This approach explicitly takes into account the interaction between the carriers in the CNT and the molecular dipole moment leading to the induction of an polarization at the surface of the tube and resulting in a clear reduction of the initial molecular dipole moment. The details will be published in a future publication [25]. We obtain $d_{MC-CNT} = 9.7$ D for merocyanine- and $d_{SP-CNT} = 5.0$ D for spiropyran-functionalized CNTs. The corresponding orientation of the dipole moment with respect to the CNT axis is given by the angle $\alpha_{MC-CNT} = 10.8^\circ$ and $\alpha_{SP-CNT} = 32.8^\circ$ [25]. The distance of the attached molecule to the CNT surface is given by the Van der Waals radius.

Once we have determined the Hamilton operator including the matrix elements and the functionalization parameters, we can apply the Heisenberg equation of motion [26] and derive many-particle Bloch equations for arbitrary hybrid nanostructures [13]. They consist of a coupled system of differential equations for the occupation probabilities $\rho^{\lambda}_{\boldsymbol{k}} = \langle a^{+}_{\lambda\boldsymbol{k}} a_{\lambda\boldsymbol{k}} \rangle$ and the microscopic polarization $p_{\boldsymbol{k}} = \langle a^{+}_{v\boldsymbol{k}} a_{c\boldsymbol{k}} \rangle$, which is a measure for the transition probability between the valence ($\lambda = v$) and the conduction band ($\lambda = c$), cp. Fig. 1b. Since we are interested in describing a linear absorption spectrum, the driving field is considered to be small resulting in a negligible change of the occupation. As a result, the optical response is determined only by the microscopic polarization, i.e. the absorption coefficient is given by

$$\alpha(\omega) \propto \omega \mathrm{Im}\chi(\omega) \propto \sum_{k} \frac{M_{vc}(k)\mathrm{Im}p_k(\omega)}{\omega A(\omega)}. \tag{3}$$

The coupling between the excitons in the CNT and the external molecular dipole moment couples the microscopic polarization to the inhomogeneous transitions $\sigma^{vc}_{k_1k_2} = \langle a^{+}_{vk_1} a_{ck_2} \rangle$ with a momentum transfer $(k_1 - k_2)$, cp. Fig. 1b. The dynamics of $\sigma^{vc}_{k_1k_2}$ is given by

$$\hbar\dot{\sigma}^{vc}_{k_1k_2} = -i(\tilde{\varepsilon}_{k_1k_2} - i\gamma)\sigma^{vc}_{k_1k_2} + i\tilde{\Omega}_{k_1k_2} - i\sum_{k'}(g^{cc}_{k_2k'}\sigma^{vc}_{k_1k'} - g^{vv}_{k'k_1}\sigma^{vc}_{k'k_2}), \tag{4}$$

where $\tilde{\varepsilon}_{k_1k_2} = (\varepsilon_{ck_2} - \varepsilon_{vk_1}) - \sum_{k'} V_{e-e}(k', k_1, k_2)$ is the band gap energy renormalized due to the repulsive electron-electron contribution $V_{e-e}(k', k_1, k_2)$ and where $\tilde{\Omega}_k(t) = \frac{e_0\hbar}{m_0} M_{cv}(k)A(t)\delta_{k_1,k_2} - \sum_{k'} V_{e-h}(k', k_1, k_2)p_{k'}(t)$ is the Rabi frequency renormalized due to the attractive electron-hole interaction $V_{e-h}(k', k_1, k_2)$. For more details on the analytic calculation of the Coulomb matrix elements using tight-binding wave functions and applying a regularized Coulomb potential see Refs. [27, 20, 28]. In the limiting case of $k_1 = k_2$, (4) contains the contribution of the microscopic polarization $p_{\boldsymbol{k}} = \sigma^{vc}_{kk}$, which turns out to be crucial for the dynamics of $\sigma^{vc}_{k_1k_2}$. The phenomenological parameter γ in (4) influences the peak width in the absorption spectrum accounting for the dephasing by scattering contributions beyond the Hartree-Fock approximation.

3. Experimental approach

In order to non-covalently attach the spiropyran-based switch to the CNT sidewall, we exploit a compound already used in [29]. It consists of of a pyrene fragment (which has been proven to efficiently stick on the nanotubes sidewalls [30]) attached as an anchoring group to the spiropyran moiety via a flexible linker. The structure of the compound as well as its chemo-physical characterization can be found in Ref. [29]. CoMoCAT nanotubes, produced by SouthWest NanoTechnologies (SWeNT, SG 76), all belonging to the same production batch were used for this experiment. The tubes have a diameter of (0.9 ± 0.3) nm and a high aspect ratio (1000). THF suspensions of our switching compound were prepared setting the molarity to 5 μM. The solution was transparent and exhibited no absorption in the visible. This implies that for THF at room temperature the switch was stable in the ring-closed spiropyran form. As a matter of fact, for the used solvent at the RT, there is no need of visible light illumination in order to induce the mero-to-spiro back isomerization, as the kinetics of the thermally driven back-isomerization takes place over a timescale comparable to the light induced one. [29] Therefore, in the experiment performed in this work, we left the sample in darkness in order to induce the mero-to-spiro back-isomerization. In order to compare to the theory and get the spectra of "pristine" tubes , we exploited 4-(1-Pyrenyl)butyric acid (PBA, CAS n.3443-45-6), which shares the same properties of our switching compound, apart from the obvious lack of the spiropyran switching moiety attached to its end.

CoMoCAT tubes were added to the solution with a starting concentration of 0.01 g/L. We treated the mixture with a tip sonicator (Bandelin SonoPlus HD 2070) at a power of 60 W and cycles of 0.5 s. After one hour the suspensions were centrifuged (Hettig Mikro 220R centrifuge) at 3500 g at 27°C for 60 min. The collected supernatant was used for the experiments. UV light source for inducing the dipole switching dynamics was a hand-held UV lamp emitting at 365 nm. UV/Vis measurements were performed with the Evolution Array Spectrophotometer by Thermo-Fisher, wavelength range 270-1100 nm.

4. Excitonic absorption spectra

First, we apply the introduced theoretical approach to determine the excitonic absorption coefficient $\alpha(\omega)$ for the exemplary pristine (10,0) zigzag carbon nanotube. Then, we calculate the spectrum of the same nanotube after the functionalization with spiropyran- and merocyanine molecules, respectively. The Bloch equation in (4) is evaluated within the Runge Kutta algorithm to obtain the temporal dynamics of the microscopic polarization $p_k(t)$ and the inhomogeneous transitions $\sigma^{vc}_{k_1k_2}(t)$. Once we have these quantities, we can easily determine $\alpha(\omega)$, cp. (3).

Figure 2 illustrates the energetically lowest transitions E_{11} in the absorption spectrum of the (10,0) nanotube before and after the functionalization. The absorption peak has a Lorentzian shape reflecting the excitonic character of the transition. Furthermore, the calculations predict a red-shift of the transition energy in the spectra of functionalized CNTs. This shift strongly depends on the molecular dipole moment and its orientation. Inserting

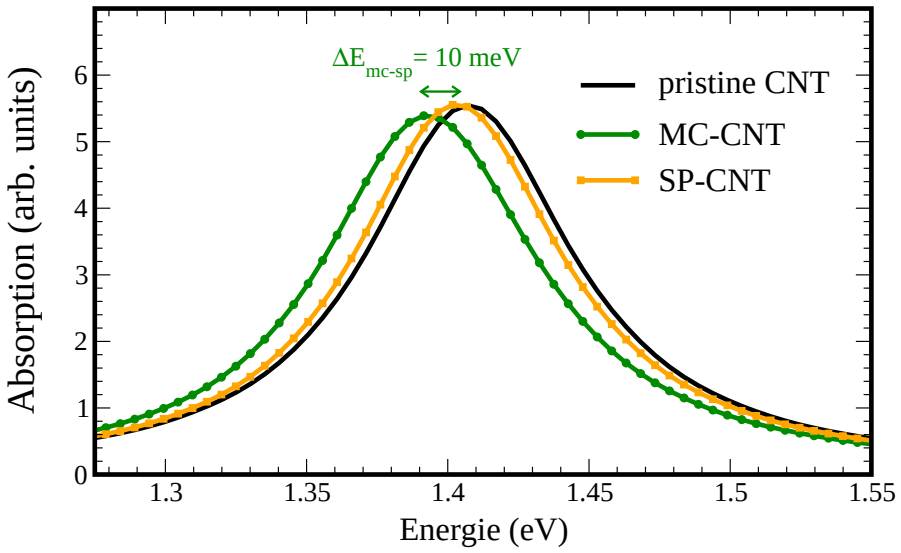

Figure 2. Theory: Excitonic absorption spectrum of the pristine, spiropyran- (SP-CNT), and merocyanine-functionalized exemplary (10,0) zigzag nanotube (MC-CNT) illustrating the energetically lowest transition E_{11}. The MC-CNT shows a clear red-shift of the transition energy due to the strong exciton-dipole interaction. The spectrum of the SP-CNT is only slightly changed in comparison to the pristine nanotube resulting in a difference of about 10 meV between the transition energies in the spectrum of MC- and SP-functionalized carbon nanotubes.

the values obtained within ab initio calculations [25], we obtain a red-shift of approximately 15 meV for merocyanine- and of < 5 meV for spiropyran-functionalized CNTs. As a result, there is a difference of about 10 meV between MC- and SP-CNTs implying the possibility of an optical read-out of spiropyran-based molecular switches on CNT substrates. The observed red-shift is due to the coupling of excitons in the CNT with the molecular dipole moment. The strength of this interaction is given by the matrix element g_{l_1,l_2}. Figure 3 shows the intraband matrix element $g^{\lambda\lambda}_{kk'}$ as a function of the momentum transfer k for an exemplary $k' = 0$. We chose the dipole moment and the dipole orientation for MC- and SP-CNTs as obtained within ab initio calculations [25]. We observe a clearly stronger matrix element in the case of nanotubes functionalized with merocyanine molecules reflecting their larger dipole moment. The strength and in particular the shape of the coupling element also depend on the dipole orientation α with respect to the CNT axis. The dashed lines in Fig. 3 show the two limiting cases of parallel ($\alpha = 0°$) and perpendicular ($\alpha = 90°$) orientation. For parallel dipoles, we observe that the coupling is zero for processes with vanishing momentum transfer, whereas for perpendicular dipoles the coupling reaches its maximal value for $k = 0$. This behavior reflects the dumbbell-like shape of the dipole potential. As a result, to obtain a maximal red-shift in the absorption spectrum, it would be advantageous to influence the orientation of the molecular dipole moment in the direction perpendicular to the CNT axis.

Now, we experimentally measure the absorption spectrum of a sample of carbon nanotubes before and after the functionalization with spiropyran molecules, cp. Fig. 4a. For pristine CNTs (i.e. coated with PBA) we observe a symmetric Lorentz-shaped peak at 1.678

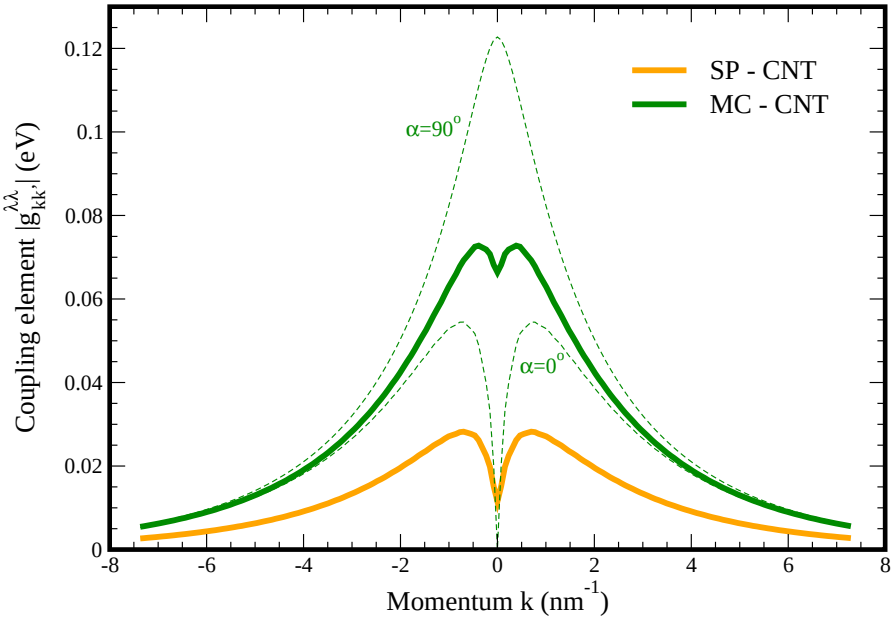

Figure 3. Absolute value of the intraband exciton-dipole coupling element $g^{\lambda\lambda}_{kk'=0}$ as a function of the momentum transfer k for spiropyran- (SP-CNT) and merocyanine-functionalized carbon nanotube (MC-CNT). The dipole moment d and the dipole orientation α (with respect to the CNT axis) are calculated in ab-initio calculations yielding $d_{MC-CNT} = 9.7$ D, $\alpha_{MC-CNT} = 10.8^\circ$ and $d_{SP-CNT} = 5.0$ D, $\alpha_{SP-CNT} = 32.8^\circ$. The dashed line shows the coupling element for the two limiting cases of the parallel ($\alpha = 0\circ$) and the perpendicular ($\alpha = 90^\circ$) dipole orientation.

eV suggesting an excitonic transition. Within a PLE map, we identify the (9,4) nanotube to be predominant in the monitored spectral window [29]. The orange peak, labeled as SP-CNT in Fig. 4a, corresponds to the transition energy in the $(9,4)$ nanotube functionalized with the dipole switch compound in the spiropyran form. Under continuous exposure to the UV radiation, the compound switches from the spiro- to the mero- form. The green, labeled as MC-CNT in Fig. 4a, corresponds to the absorption peak of the nanotube coated with the dipole switch compound in the merocyanine form. Here, we find a red-shift of the transition energy by around 6 meV with respect to the pristine CNT. In contrast, there is no measurable change in the case of SP-CNTs. This is in good agreement with our theoretical predictions. In experiment, the red-shift is quantitatively smaller probably accounting for a larger molecule-CNT distance due to anchor molecules used in the process of functionalization. Furthermore, the molecules will not be perfectly aligned along the CNT surface as assumed in ab initio calculations. The change of the position of the absorption peak during the switching dynamics can be monitored in real-time over a period of time. Figure 4b shows the temporal evolution of the red-shift, when ultraviolet light is switched on inducing the isomerization of the spiropyran molecule into the open merocyanine form. We observe a continuous increase of the red-shift reflecting the gradual switching processes of the spiropyran molecules. After the light is switched off and the sample is located in the dark, the back-isomerization is initiated and the red-shift starts to decrease again. It takes around 100 seconds, until the molecule is completely

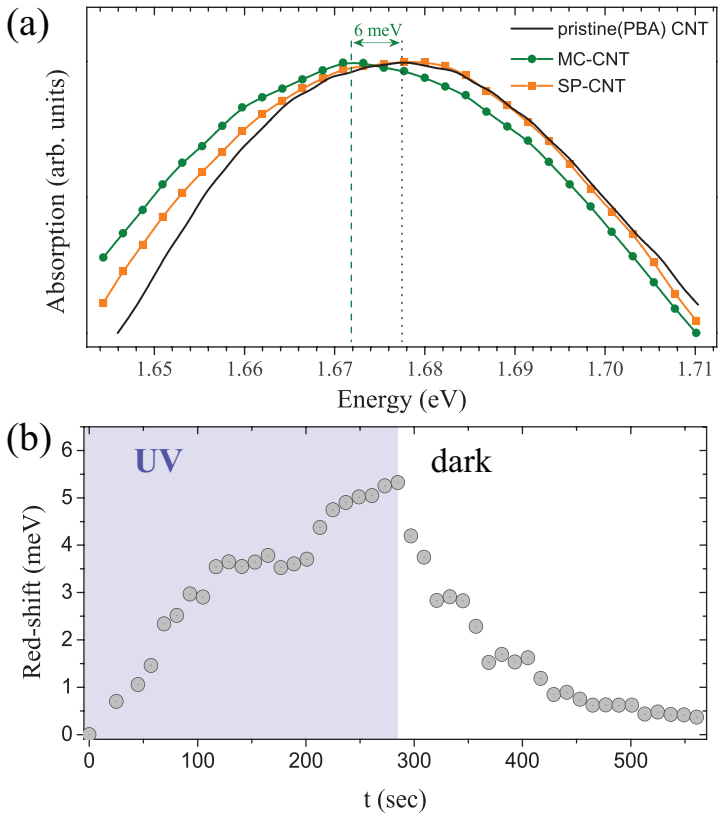

Figure 4. Experiment: a) Absorption spectrum of the pristine (i.e. coated with PBA), merocyanine, and spiropyran-functionalized carbon nanotubes illustrating a red-shift for MC-CNTs of about 6 meV. The spectrum of SP-CNTs remains basically unchanged. b) Temporal dynamics of the observed red-shift, when ultraviolet light is switched on and off inducing the isomerization between the spiropyran and merocyanine form.

switched back into the closed spiropyran form.

5. Conclusions

In summary, we have theoretically and experimentally investigated the absorption spectrum of spiropyran-functionalized carbon nanotubes. We observe a red-shift strongly depending on the conformation of the attached molecule: For the open merocyanine form, which is characterized by a large dipole moment, we observe a red-shift of the energetically lowest transition energy by about 15 meV. This shift reflects the interaction between the excitons in the carbon nanotube and the external molecular dipole field. In contrast, in the case of the closed spiropyran form, the absorption spectrum is only slightly red-shifted reflecting the smaller molecular dipole moment. This suggests the possibility of an optical read-out of a spiropyran-based molecular switch. Our theoretical predictions are in good agreement with experimental results confirming the predicted red-shift in the absorption spectra of functionalized nanotubes. Furthermore, our calculations show that the observed red-shift strongly depends on the dipole moment and the dipole orientation. As a result, it could

be optimized with regard to an optical read-out by aligning the molecular dipole moment perpendicular to the nanotube axis, which yields the strongest dipole-induced substrate-molecule coupling.

Acknowledgments

We acknowledge financial support by the Deutsche Forschungsgemeinschaft through SFB 658. E. M. acknowledges funding by the Einstein Foundation.

References

[1] M. Strano, V. C. Moore, M. K. Miller, M. J. Allen, E. H. Haroz, C. Kittrell, R. H. Hauge, and R. E. Smalley. *J. Nanosci. Nanotechnol.*, 3(1):81–86, 2003.

[2] R. F. Khairutdinov, M. E Itkis, and R. C Haddon. *Nano Lett.*, 4(8):1529–1533, 2004.

[3] A Hirsch and O Vostrowsky. In *Functional Molecular Nanostructures*, volume 245 of *Top. Curr. Chem.*, pages 193–237. 2005.

[4] M Burghard. *Surf. Sci. Rep.*, 58(1-4):1–109, 2005.

[5] X. F Guo, L. M Huang, S O'Brien, P Kim, and C Nuckolls. *J. Am. Chem. Soc.*, 127(43):15045–15047, 2005.

[6] Xinjian Zhou, Jose M. Moran-Mirabal, Harold G. Craighead, and Paul L. McEuen. *Nature Nanotechnology*, 2(3):185–190, 2007.

[7] J. M. Simmons, I. In, V. E. Campbell, T. J. Mark, F. Léonard, P. Gopalan, and M. A. Eriksson. *Phys. Rev. Lett.*, 98(8):086802, Feb 2007.

[8] Miriam Del Valle, Rafael Gutirrez, Carlos Tejedor, and Gianaurelio Cuniberti. *Nature Nanotechnology*, 2(3):176–179, 2007.

[9] A. Jorio, M. S Dresselhaus, and G. Dresselhaus. *Carbon nanotubes: advanced topics in the synthesis, structure, properties and applications*. Springer, Berlin, 2008.

[10] Xinjian Zhou, Thomas Zifer, Bryan M. Wong, Karen L. Krafcik, Francois Leonard, and Andrew L. Vance. *Nano Lett.*, 9(3):1028–1033, 2009.

[11] Elisa Del Canto, Kevin Flavin, Manuel Natali, Tatiana Perova, and Silvia Giordani. *Carbon*, 48(10):2815–2824, 2010.

[12] Jamie Whelan, Dalia Abdallah, James Wojtyk, and Erwin Buncel. *J. Mater. Chem.*, 20(27):5727–5735, 2010.

[13] E. Malić, C. Weber, M. Richter, V. Atalla, T. Klamroth, P. Saalfrank, S. Reich, and A. Knorr. *Phys. Rev. Lett.*, 106:097401, 2011.

[14] G Berkovic, V Krongauz, and V Weiss. *Chem. Rev.*, 100(5):1741–1753, 2000.

[15] Seokho Lim and Noejung Park. *Appl. Phys. Lett.*, 95(24), 2009.

[16] S. Reich, J. Maultzsch, C. Thomsen, and P. Ordejón. *Phys. Rev. B*, 66:035412, 2002.

[17] Ermin Malić, Matthias Hirtschulz, Frank Milde, Andreas Knorr, and Stephanie Reich. *Phys. Rev. B*, 74(19):195431, 2006.

[18] A. Grüneis, R. Saito, G. G. Samsonidze, T. Kimura, M. A. Pimenta, A. Jorio, A. G. SouzaFilho, G. Dresselhaus, and M. S. Dresselhaus. *Phys. Rev. B*, 67:165402, 2003.

[19] Ermin Malić, Matthias Hirtschulz, Frank Milde, Yang Wu, Janina Maultzsch, Tony F. Heinz, Andreas Knorr, and Stephanie Reich. *Phys. Rev. B*, 77(4):045432, 2008.

[20] Matthias Hirtschulz, Frank Milde, Ermin Malić, Stefan Butscher, Christian Thomsen, Stephanie Reich, and Andreas Knorr. *Phys. Rev. B*, 77(3):035403, 2008.

[21] P Ordejon, E Artacho, and JM Soler. *Phys. Rev. B*, 53(16):10441–10444, 1996.

[22] J. M. Soler, E. Artacho, J. D. Gale, A. Garcia, J. Junquera, P. Ordejon, and D. Sanchez-Portal. *J. Phys.: Condens. Matter*, 14(11):2745–2779, 2002.

[23] Guillermo Roman-Perez and Jose M. Soler. *Phys. Rev. Lett.*, 103(9), 2009.
[24] M. Baldoni, A. Sgamellotii, and F. Mercuri. *Org. Lett.*, 9:4267, 2007.
[25] Ermin Malić and Carlos F. Sanz-Navarro and Pablo Ordejón. 2012.
[26] H. Haug and S. W. Koch. *Quantum Theory of the Optical and Electronic Properties of Semiconductors*. World Scientific, Singapore, 2004.
[27] Ermin Malić, Matthias Hirtschulz, Frank Milde, Janina Maultzsch, Stephanie Reich, and Andreas Knorr. *Phys. Stat. Solidi (B)*, 245:2155, 2008.
[28] Ermin Malić, Janina Maultzsch, Stephanie Reich, and Andreas Knorr. *Phys. Rev. B*, 82(3):035433, 2010.
[29] A. Setaro, P. Bluemmel, C. Maity, S. Hecht, and S. Reich, *submitted*
[30] R. J. Chen, Y. Zhang, D. Wang, and H. Dai. *Journal of the American Chemical Society*, 123(16):3838, 2001.